IOP Conf. Series: Materials Science and Engineering **145** (2016) 042033 doi:10.1088/1757-899X/145/4/042033

A numerical solution to the cattaneo-mindlin problem for viscoelastic materials

S Spinu[1, 2] **and D Cerlinca**[1, 2]
[1]Department of Mechanics and Technologies, Stefan cel Mare University of Suceava, 13th University Street, 720229, Romania
[2]Integrated Center for Research, Development and Innovation in Advanced Materials, Nanotechnologies, and Distributed Systems for Fabrication and Control (MANSiD), Stefan cel Mare University, Suceava, Romania

E-mail: sergiu.spinu@fim.usv.ro

Abstract. The problem of the frictional mechanical contact with slip and stick, also referred to as the Cattaneo-Mindlin problem, is an important topic in engineering, with applications in the modeling of particle-flow simulations or in the study of contact between rough surfaces. In the frame of Linear Theory of Elasticity, accurate description of the slip-stick contact can only be achieved numerically, due to mutual interaction between normal and shear contact tractions. Additional difficulties arise when considering a viscoelastic constitutive law, as the mechanical response of the contacting materials depends explicitly on time. To overcome this obstacle, an existing algorithm for the purely elastic slip-stick contact is coupled with a semi-analytical method for viscoelastic displacement computation. The main advantage of this approach is that the contact model can be divided in subunits having the same structure as that of the purely elastic frictionless contact model, for which a well-established solution is readily available. In each time step, the contact solver assesses the contact area, the pressure distribution, the stick area and the shear tractions that satisfy the contact compatibility conditions and the static force equilibrium in both normal and tangential directions. A temporal discretization of the simulation windows assures that the memory effect, specific to both viscoelasticity and friction as a path-dependent processes, is properly replicated.

1. Introduction

The tribological contacts in industrial mechanisms undergo oscillating tangential displacements, leading to a dramatic decrease of service lifetime of the contacting machine elements by fretting wear and fretting fatigue. From a mechanical point of view, the Cattaneo-Mindlin problem is treated in the frame of Contact Mechanics by incorporating the Linear Theory of Elasticity, but derivation of a closed-form solution is impeded by the coupling between normal and tangential effects [1]. The problem model becomes even more complicated by integration of viscoelasticity, due to introduction of time as a new parameter. With complete analytical solutions lacking in both elasticity and viscoelasticity, a numerical study is expected to advance the understanding of the slip-stick contact and to provide assistance to the design of machine elements with improved load-carrying capacity.

The method employed in this paper is referred in the literature as semi-analytical (SAM) [2], and its strong point is that domain discretization is limited to a surface region of the contacting body, as opposed to finite element analysis (FEA), in which the meshing of the entire bulk is required. This

translates to a dramatic increase in computational efficiency. It is asserted in [2] that SAM can be employed to solve a three-dimensional contact problem with the computational resources required in FEA for a two-dimensional contact process.

The treatment of slip-stick contact problems using SAM originated in the work of Gallego, Nélias and Jacq [3], who solved repeatedly the contact model in the normal direction while accounting for the change in conformity due to wear. Chen and Wang [4] advanced a numerical model for the partial slip non-conforming contact considering tangential tractions. This model was later extended in [5], by considering a supplementary torsional moment, and in [6], by including the heterogeneity of elastic layered half-spaces. Further iterations proved the necessity of incremental load application due to the irreversibility of friction as a dissipative process, as reported by Gallego, Nélias and Deyber [7], and by Spinu and Glovnea [8]. The study of the memory effect in the fretting contact between dissimilarly elastic materials was conducted by Spinu and Frunza [9].

Application of SAM to viscoelastic contact problems is more recent, and results are restricted to frictionless contact scenarios. The indentation of a viscoelastic half-space using the Matrix Inversion Method was investigated in [10]. A robust semi-analytical method for contact modelling of polymer-based materials was proposed in [11]. The multi-indentation of a viscoelastic half-space by rigid bodies using a two-scale iterative method was analysed in [12]. More recently, Spinu [13] advanced an improved algorithm for the simulation of frictionless contact problems.

The main goal of this paper is to extend the SAM-based elastic contact model to viscoelastic materials. To this end, existing algorithms for the Cattaneo-Mindlin problem and for viscoelastic displacement computation are adapted and combined in an incremental iterative process, aiming to accurately reproduce the frictional contact process. The use of state-of-the-art numerical tools allows implementation of fine spatial and temporal meshes, resulting in well-converged numerical solutions.

2. The contact model

The main difficulty in solving the contact problem consist in the fact that neither the contact area, nor the stick area, nor the contact tractions are known in advance. A trial-and-error approach is implemented since the work of [14], but the resulting iterative process infer integration of arbitrary functions (contact tractions distributions) over irregular domains (contact or stick area). As this cannot generally be performed analytically, numerical integration assisted by influence coefficients is preferred. The basic principles of contact problem discretization are briefly discussed in this section.

The initial composite contact geometry $hi(x_1, x_2)$ is conveniently described in a Cartezian coordinate systems having its x_1 and x_2-axes contained in the common plane of contact (i.e. the plane passing through the first point of contact, chosen as to separate best the bounding surfaces). The direction of the x_3-axis will be referred to as the normal direction, while the other two are tangential directions. Forces and moments transmitted through the contact have components along all three axes: the normal force W, the tangential force $\mathbf{T}(T_1, T_2)$, the bending (or flexing) moments M_1, M_2 and the torsional moment M_3. Under load, the contacting bodies deform unless assumed rigid, exhibiting relative viscoelastic displacements u_i, and move relative to each other as rigid-bodies with translations ω_i and rotations ϕ_i, with $i = 1,2,3$. Once a non-vanishing contact area A is established, contact tractions occur, i.e. pressure p in the normal direction and shear traction $\mathbf{q}(q_1, q_2)$ in the tangential direction. The works of Cattaneo [15] and Mindlin [16] prove that the full-sticking contact cannot be solved in the Frame of Linear Theory of Elasticity, as it leads to infinite stresses at the boundary of the contact area. The full-slip contact is trivial, as shear tractions are related to pressure through Coulomb's law on all contact area. The main goal of this work is the study of the partial slip (i.e. slip-stick) contact, in which the contacting bodies are globally sticking due to a stick area S, but a peripheral region of slip occurs to release the otherwise infinite tractions on the contact boundary. In the problem model, μ is the frictional coefficient, $A - S$ the slip region, and $\mathbf{s}(s_1, s_2)$ the relative slip distances, as discussed in [17].

The SAM-based resolution of the slip-stick contact problem relies on considering continuous distributions as piecewise constant over a rectangular mesh P established in the common plane of contact, enclosing the contact area at any moment in the loading history. Only a small surface domain (i.e. the contact vicinity) of the contacting bodies needs to be meshed. It is convenient to align the directions of the grid sides with those of the Cartesian coordinate system. The elementary cell area $\Delta = \Delta_1\Delta_2$ depends on the grid steps Δ_i in the direction of $\vec{x}_i$, $i = 1,2$. The grid control points, i.e. the centres of the resulting rectangular patches, are indexed by a pair of indices (i, j), with $1 \le i < N_1$ and $1 \le i < N_2$. Any continuous distribution is approximated by a series of discrete values computed in the control points. This spatial discretization is competent in purely elastic contact problems, but it cannot handle by itself path-dependent processes, like friction. The latter cases require incremental load application, as described in [7]; however, the time parameter needs not be explicitly considered. Simulation of the viscoelastic contact process, on the other hand, require the time parameter to be unequivocally included, as the mechanical response of the viscoelastic material depend explicitly on time. A uniform temporal mesh of step Δ_t, with N_t time steps, completes the problem model, adding a third argument to all problem parameters, e.g. $p(i, j, k)$ is the discrete counterpart of $p(x_1', x_2', t')$, with $x_1' = i\Delta_1$, $x_2' = j\Delta_2$, $t' = k\Delta_t$, and denotes the elementary pressure in the cell (i, j) of the spatial mesh, achieved after k time steps. Parameters having two arguments depend only on spatial localization, while those with one argument depend only on time.

In this framework, the contact model can be subdivided into two components that have the same structure and consequently can be solved using the same type of algorithm. However, as shown in the next sections, the two submodels cannot be solved independently, but rather stabilized one with respect to the other in an iterative approach. The normal contact (NC) submodel consists in equations (1), (3) and (5), describing the contact behavior in the normal direction, while the tangential contact (TC) submodel comprises equations (2), (4) and (6) for the tangential direction:

1. The static force and moment equilibrium:

$$W(k) = \Delta \sum_{(i,j)\in A(k)} p(i, j, k); M_1(k) = \Delta \sum_{(i,j)\in A(k)} p(i, j, k)x_2(i, j); M_2(k) = \Delta \sum_{(i,j)\in A(k)} p(i, j, k)x_1(i, j); \quad (1)$$

$$T_n(k) = \Delta \sum_{(i,j)\in A(k)} q_n(i, j, k), n = 1,2; M_3(k) = \Delta \sum_{(i,j)\in A(k)} \left[q_2(i, j, k)x_1(i, j) - q_1(i, j, k)x_2(i, j)\right]. \quad (2)$$

2. The geometrical condition of deformation:

$$h(i, j, k) = hi(i, j) + u_3(i, j, k) - \omega_3(k) - \phi_1(k)x_2(i, j) - \phi_2(k)x_1(i, j), (i, j) \in P; \quad (3)$$

$$\begin{bmatrix} s_1(i, j, k) - s_1(i, j, k-1) \\ s_2(i, j, k) - s_2(i, j, k-1) \end{bmatrix} = \begin{bmatrix} u_1(i, j, k) - u_1(i, j, k-1) \\ u_2(i, j, k) - u_2(i, j, k-1) \end{bmatrix} - \begin{bmatrix} \omega_1(k) - \omega_1(k-1) \\ \omega_2(k) - \omega_2(k-1) \end{bmatrix} - \left(\phi_3(k) - \phi_3(k-1)\right)\begin{bmatrix} x_2(i, j) \\ x_1(i, j) \end{bmatrix}, \quad (i, j) \in A(k). \quad (4)$$

3. The contact complementarity conditions:

$$\begin{cases} p(i, j, k) > 0 \quad \text{and} \quad h(i, j, k) = 0, \quad (i, j) \in A(k); \\ p(i, j, k) = 0 \quad \text{and} \quad h(i, j, k) > 0, \quad (i, j) \in P - A(k); \end{cases} \quad (5)$$

$$\begin{cases} \|\mathbf{q}(i, j, k)\| \le \mu p(i, j, k) \quad \text{and} \quad \|\mathbf{s}(i, j, k) - \mathbf{s}(i, j, k-1)\| = 0, (i, j) \in S(k); \\ \|\mathbf{q}(i, j, k)\| = \mu p(i, j, k) \quad \text{and} \quad \|\mathbf{s}(i, j, k) - \mathbf{s}(i, j, k-1)\| > 0, (i, j) \in A(k) - S(k). \end{cases} \quad (6)$$

3. Viscoelastic displacement computation

A semi-analytical method for computation of normal displacement in linear viscoelastic materials was recently advanced by Spinu and Gradinaru [18]. As shown by the geometrical condition of deformation (3) and (4), assessment of displacement field induced in the viscoelastic material by an arbitrary history of surface tractions in a contact process is essential in solving the contact problem. By adopting the assumption of linearity in viscoelastic response (reasonable in the frame of small strain theory), the use of Boltzmann superposition theory is authorized, allowing displacement to be obtained as the superposition of a series of small changes in contact tractions, i.e. $p(i,j,k)-p(i,j,k-1)$ and $\mathbf{q}(i,j,k)-\mathbf{q}(i,j,k-1)$. By extending the formula derived in [18], the linear viscoelastic displacement induced by an arbitrary, yet known, history of distributions of contact tractions, both normal and shear, results as:

$$\begin{bmatrix} u_1(i,j,k) \\ u_2(i,j,k) \\ u_3(i,j,k) \end{bmatrix} = \sum_{n=1}^{N_t}\sum_{\ell=1}^{N_1}\sum_{m=1}^{N_2} \begin{bmatrix} KV_{11}(i-\ell,j-m,k-n) & KV_{12}(i-\ell,j-m,k-n) & KV_{13}(i-\ell,j-m,k-n) \\ KV_{21}(i-\ell,j-m,k-n) & KV_{22}(i-\ell,j-m,k-n) & KV_{23}(i-\ell,j-m,k-n) \\ KV_{31}(i-\ell,j-m,k-n) & KV_{32}(i-\ell,j-m,k-n) & KV_{33}(i-\ell,j-m,k-n) \end{bmatrix} \cdot \begin{bmatrix} q_1(\ell,m,n)-q_1(\ell,m,n-1) \\ q_2(\ell,m,n)-q_2(\ell,m,n-1) \\ p(\ell,m,n)-p(\ell,m,n-1) \end{bmatrix}, \quad \text{where} \tag{7}$$

$$\begin{bmatrix} KV_{11} & KV_{12} & KV_{13} \\ KV_{21} & KV_{22} & KV_{23} \\ KV_{31} & KV_{32} & KV_{33} \end{bmatrix} \equiv \begin{bmatrix} KV_{11}^{(2)}+KV_{11}^{(1)} & KV_{12}^{(2)}+KV_{12}^{(1)} & KV_{13}^{(2)}-KV_{13}^{(1)} \\ KV_{21}^{(2)}+KV_{21}^{(1)} & KV_{22}^{(2)}+KV_{22}^{(1)} & KV_{23}^{(2)}-KV_{23}^{(1)} \\ KV_{31}^{(2)}-KV_{31}^{(1)} & KV_{32}^{(2)}-KV_{32}^{(1)} & KV_{33}^{(2)}+KV_{33}^{(1)} \end{bmatrix}. \tag{8}$$

Here, $KV_{\zeta\xi}^{(\psi)}(i-\ell,j-m,k-n)$ denotes the viscoelastic influence coefficient, expressing the displacement in the direction of $\vec{x}_\zeta$, induced in the elementary patch (i,j) of the body ψ, at the time step k, by a uniform contact traction of $1/(\Delta_1\Delta_2)$ Pa that acted in the patch (ℓ,m), along direction of $\vec{x}_\xi$, in the n^{th} time step, with $n\le k$, $\zeta,\xi=1,2,3$, and $\psi=1,2$. As shown in [18], the viscoelastic influence coefficient $KV_{\zeta\xi}^{(\psi)}$ can be derived based on its elastic counterpart $K_{\zeta\xi}^{(\psi)}$:

$$KV_{\zeta\xi}^{(\psi)}(i-\ell,j-m,k-n)=E^{(\psi)}(1+\nu^{(\psi)})^{-1}\Phi^{(\psi)}\left((k-n)\Delta_t\right)K_{\zeta\xi}^{(\psi)}(i-\ell,j-m), \tag{9}$$

where $E^{(\psi)}$, $\nu^{(\psi)}$ and $\Phi^{(\psi)}(t)$ are the Young modulus, the Poisson's ratio and the creep compliance function of the contacting body ψ, respectively, with $\psi=1,2$ and $\zeta,\xi=1,2,3$. The viscoelastic influence coefficient was essentially obtained by replacing the elastic modulus in the elastic influence coefficient with the viscoelastic creep compliance, as detailed in [18]. The derivation of the purely elastic influence coefficients for frictional contact problems is discussed in detail elsewhere [19].

4. Algorithm description

The difficulty in achieving an analytical solution to the Cattaneo-Mindlin problem for viscoelastic materials stems from three facts. Firstly, the contact area, as well as the slip / stick boundary, is a priori unknown and keep changing with time in the course of the contact process. Secondly, the NC and the TC cannot be solved independently, as the displacement fields entering the geometrical conditions of deformation (3) and (4) result by superposing the contributions of both normal and shear tractions. In other words, solution of the NC is required to solve the TC and vice versa. Thirdly, the slip-stick contact simulation relies on contact evolution in the past period of time. Indeed, computation of surface normal or tangential displacement is based on both normal and shear tractions developed

during the contact process. To overcome each of these obstacles, an additional level of iteration is implemented, resulting in a three level nested loop.

The innermost loop will be referred to as the uncoupled contact problem, which can be in the normal (UNC) of in the tangential (UTC) direction. The intermediate loop iterates between the UNC and the UTC to obtain the instantaneous contact state (IC), namely the solution that couples the UNC and the UTC. The outer loop replicates the viscoelastic slip-stick contact process by computing a series of ICs at each increment in the temporal mesh. A similar type of three-level iteration was implemented by Spinu and Glovnea [8] in the study of slip-stick elastic contact, therefore only the novelty features will be detailed in this paper.

By integrating the viscoelastic constitutive law into the slip-stick contact model, replication of the process path by incremental load application alone is no longer possible. Indeed, in the purely elastic slip-stick contact, no parameter depends explicitly on time, and the path-dependent frictional process is accurately reproduced as long as the tangential load is applied in sufficiently small increments. The outcome of the elastic slip-stick contact is independent of the simulation time window, as the response of the contacting material appears to be time-independent on condition that load varies slowly. As opposed to the viscoelastic case, when the stress and strain state in the contacting bodies depend not only on the past evolution of the load, but also on the time interval in which the loading program was applied. In other words, the time increments in the outer level of discretization should be small enough to assure not only that the tangential load is applied in small steps (as required by the path-dependent frictional process), but also that the mechanical response of the viscoelastic body does not vary significantly from one time increment to another.

From this point forward, the spatial localization of displacement will be omitted for brevity. The displacement in the k^{th} time increment results as the contribution of the current and past contact tractions, both normal and shear, all unknown, i.e. $\mathbf{u}(k)=\mathbf{u}(p(1),...,p(k),\mathbf{q}(1),...,\mathbf{q}(k))$; whereas, based on the state-of-the-art in computational contact mechanics, we can only solve the uncoupled contact problems with just one unknown contact traction, i.e. either when $\mathbf{u}(k)=\mathbf{u}(p(k))$, or when $\mathbf{u}(k)=\mathbf{u}(\mathbf{q}(\mathrm{k}))$. The problem solution is achieved in this paper by means of three iterative levels. At the intermediate level (previously referred to as an IC), the historical contact tractions are assumed known, and therefore the only unknowns are the current tractions, i.e. $\mathbf{u}(k)=\mathbf{u}(p(k),\mathbf{q}(\mathrm{k}))$. At the inner loop level, also referred to as uncoupled contact model, only one unknown is kept, i.e. $\mathbf{u}(k)=\mathbf{u}(p(k))$ in the UNC and $\mathbf{u}(k)=\mathbf{u}(\mathbf{q}(\mathrm{k}))$ in the UTC.

Once a contact traction is assumed known in the contact solver, its contribution to the displacement field can be superimposed in the geometrical conditions of deformation (3) and (4) to the initial contact geometry, resulting in a modified initial state. The main advantage of this approach is that the resulting contact model preserves the same structure as the purely elastic frictionless contact model, for which a well-established numerical solution is readily available [20]. It was shown [8] that the latter type of algorithm can be used to solve either the UNC or the UTC. Its description is omitted in this paper for brevity.

The algorithm steps for the intermediate loop (i.e. the solution of the IC) are detailed below.

1. Acquire the historical contact tractions: $p(1),...,p(k-1),\mathbf{q}(1),...,\mathbf{q}(k-1)$.

2. Adopt the initial guess for the shear contact tractions: $\mathbf{q}(k)=\mathbf{q}(k-1)$. A vanishing increment can also be assumed, but results in slower convergence.

3. Compute the contribution of $p(1),...,p(k-1),\mathbf{q}(1),...,\mathbf{q}(k)$ to displacement and superimpose it to the initial state in the UNC.

4. Solve the UNC with only one unknown traction: $\mathbf{u}(k)=\mathbf{u}(p(k))$. Obtain $p(k)$.

5. Memorize $p(k)$ for subsequent error estimation: $p_{old}(k)\equiv p(k)$.

6. Compute the contribution of $p(1),...,p(k),\mathbf{q}(1),...,\mathbf{q}(k-1)$ to displacement and superimpose it to the initial state in the UTC.

7. Solve the UTC with only one unknown traction: $\mathbf{u}(k)=\mathbf{u}(\mathbf{q}(k))$. Obtain a better approximation for the shear tractions $\mathbf{q}(k)$ than the one assumed in step 2.

8. Obtain the next iteration for the normal tractions $p(k)$ by rerunning steps 3 and 4 with the newly computed shear tractions $\mathbf{q}(k)$.

9. Verify convergence by comparing $p(k)$ to $p_{old}(k)$. If these pressure distributions vary within an imposed precision with respect to the applied normal load, stop algorithm execution and export data. If not, resume from step 5 to perform a new iteration.

In this manner, the UNC and the UTC are solved successively, generating new iterations of $p(k)$ and of $\mathbf{q}(k)$, which converge to the solution of the IC, i.e. the couple $\left(p(k),\mathbf{q}(k)\right)$ that verifies both the UNC and the UTC simultaneously.

The simulation of the viscoelastic contact process by means of a series of instantaneous contact states is achieved in the outer loop, which consists in the following steps:

1. Solve an initial UNC to get the pressure at the beginning of the loading process $p(1)$. It should be noted that in the Cattaneo-Mindlin problem, the normal load is applied first, and the tangential load acts after the contact area is established.

2. Apply the tangential load in the time step k and solve the current IC to get $p(k)$ and $\mathbf{q}(k)$.

3. Increase k. If the end of the simulation window is reached (i.e. $k>N_t$), export data, if not, resume algorithm execution from step 2.

5. Results and discussions

The newly proposed algorithm is firstly validated by comparison with the closed-form solution detailed in [17] for the purely elastic spherical contact undergoing a fretting loop. The results are then extended by simulating the indentation of a Maxwell viscoelastic half-space by a rigid sphere. The Maxwell rheological model consists in a spring of shear modulus G in series with a dashpot of viscosity η. The creep compliance function of the Maxwell half-space is $\Phi(t)=1/(2G)(1+t/t')$, where $t'=\eta/G$ denotes the relaxation time, namely the time it takes for stress to decay by a factor equal to the Euler's number.

During a fretting contact process, it is expected that friction vary on the contact area, as well as with accumulation of debris particles resulted from additional wear. However, for validation purposes, a frictional coefficient $\mu=0.1$, uniform over all contact area and constant during load application, is assumed in this study. The proposed numerical method can equally handle mapped distributions of μ.

A steel ball of radius $R=18\,\text{mm}$ is pressed against an elastic half-space having the same elastic properties, in a step loading with a normal force $W=1\,\text{kN}$. A tangential force T, varying linearly with time between two limiting values T_{lim} and $-T_{\text{lim}}$, where $T_{\text{lim}}=0.9\mu W$, is subsequently applied. The loading history for the elastic or the viscoelastic fretting processes is depicted in figure 1, with dimensionless time defined as ratio to the length of the simulation window τ and with $t=0\,\text{s}$ the moment of the first loading. The length of the simulation window is varied with respect to the relaxation time of the Maxwell rheological model. The Hertz frictionless theory for this contact scenario predicts a central pressure $p_H=1.996\,\text{GPa}$ and a contact radius $a_H=0.489\,\text{mm}$. In figures 2 and 3, dimensionless contact tractions are defined as ratio to p_H, and dimensionless radial coordinate as ratio to a_H.

In the elastic case (figure 2), the pressure is constant and the shear contact tractions depend only on the dimensionless time, whereas, in the viscoelastic case, pressure not only varies with dimensionless time, but it is also influenced by the relaxation time of the viscoelastic rheological model. The length of the simulation window has a noticeable influence on both normal and shear contact tractions, as resulting from comparison of distributions depicted in figure 3(a) and (b).

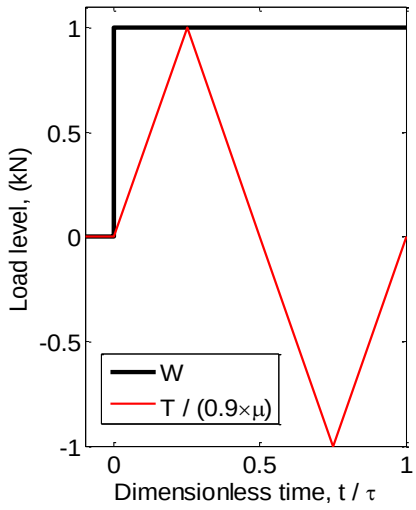

Figure 1. The loading history.

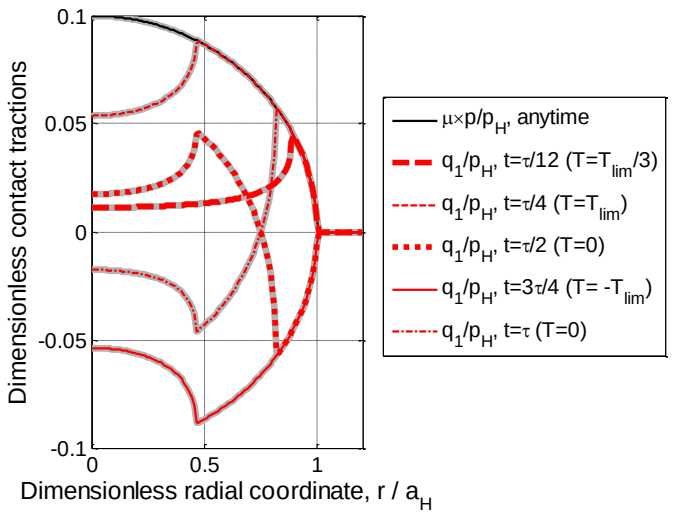

Figure 2. Program validation by simulation of a fretting loop in a purely elastic contact. The closed-form solution [17] used for comparison is displayed using grey lines.

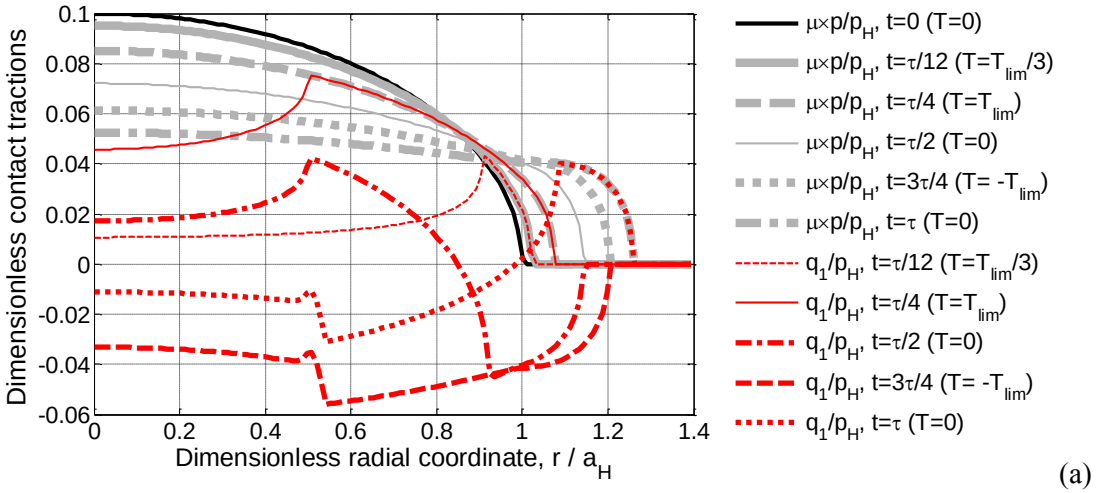

(a)

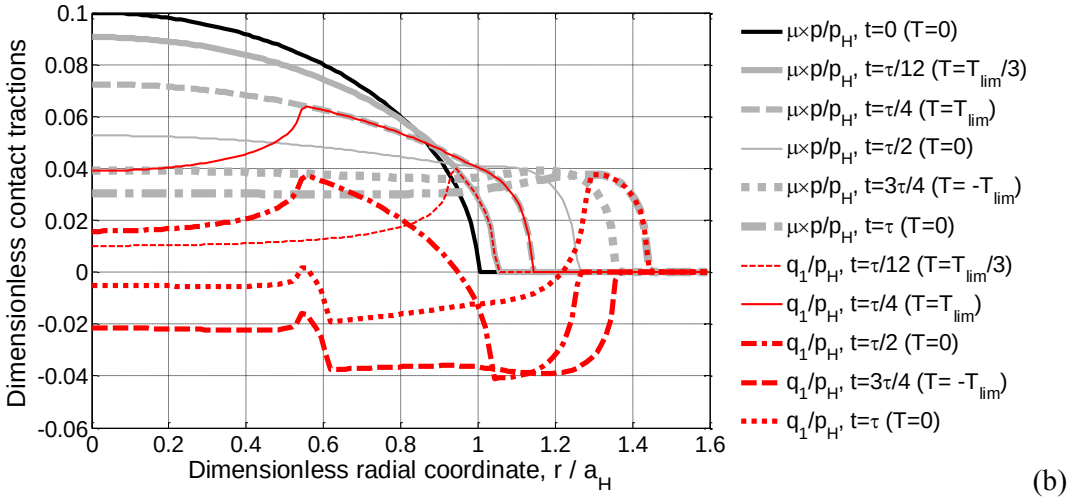

(b)

Figure 3. Contact tractions in the viscoelastic contact: (a) $\tau = t'$, (b) $\tau = 2t'$.

6. Conclusions

The numerical solution of the Cattaneo-Mindlin problem for materials with dissimilar elastic responses is extended to allow for linear viscoelastic behavior. Beside the spatial discretization specific to elastic contact problems, a temporal discretization of the simulation window is implemented, with time steps sufficiently short so that the tangential load level and the material response can be assumed constant in each step. This discrete model assures the computation of viscoelastic displacement by superposing the contributions of contact tractions in all past intervals.

The newly proposed algorithm is based on three level of iterations. The inner level solves the normal or the tangential instantaneous contact state at each time increment, i.e. the uncoupled contact problems in the normal or in the tangential direction. The intermediate level iterates between the normal and the tangential instantaneous contact tractions, stabilizing one with respect to the other and thus coupling the normal and the tangential contact models. The outer level superpose the contribution of all past increments, thus simulating the memory effect specific to both viscoelasticity and friction.

Due to its generality, this novel method is expected to provide assistance to the design of competent tribological components for practical engineering applications involving viscoelastic materials and interfacial friction.

Acknowledgement

This work was partially supported from the project “Integrated Center for Research, Development and Innovation in Advanced Materials, Nanotechnologies, and Distributed Systems for Fabrication and Control”, Contract No. 671/09.04.2015, Sectoral Operational Program for Increase of the Economic Competitiveness co-funded from the European Regional Development Fund.

References

[1] Hills D A, Nowell D and Sackfield A 1993 *Mechanics of elastic contacts* (Oxford: Butterworth-Heinemann)
[2] Renouf M, Massi F, Fillot N and Saulot A 2011 *Tribol. Int.* **44** 834
[3] Gallego L, Nélias D and Jacq C 2006 *ASME J. Tribol.* **128** 476
[4] Chen W W and Wang Q J 2008 *Mech. Mater.* **40** 936
[5] Wang Z J, Meng F M, Xiao J X and Wang W Z 2011 *P. I. Mech. Eng. J.-J. Eng.* **225** 72
[6] Wang Z J, Wang W Z, Wang H, Zhu H and Hu Y Z 2010 *ASME J. Tribol.* **132** 021403
[7] Gallego L, Nélias D and Deyber S 2010 *Wear* **268** 208
[8] Spinu S and Glovnea M 2012 *J. Balk. Tribol. Assoc.* **18** 195
[9] Spinu S and Frunza G 2015 *J. Phys.: Conf. Ser.* **585** 012007
[10] Kozhevnikov I F, Cesbron J, Duhamel D, Yin H P and Anfosso-Ledee F 2008 *Int. J. Mech. Sci.* **50** 1194
[11] Chen W W, Wang Q J, Huan Z and Luo X 2008 *ASME J. Tribol.* **133** 041404
[12] Kozhevnikov I F, Duhamel D, Yin H P and Feng Z Q 2010 *Int. J. Mech. Sci.* **52** 399
[13] Spinu S 2015 *J. Balk. Tribol. Assoc.* **21** 269
[14] Kalker J J and van Randen Y A 1972 *J. Eng. Math.* **6** 193
[15] Cattaneo C 1938 Sul contatto di due corpi elastici: distribuzione locale degli sforzi *Accademia Nazionale Lincei Rendiconti Ser. 6* **27** (Roma: L'Accademia) pp 342-348, 434-436, 474-478
[16] Mindlin R D 1949 *ASME J. Appl. Mech.* **16** 259
[17] Johnson K L 1985 *Contact Mechanics* (Cambridge: University Press)
[18] Spinu S and Gradinaru D 2015 *IOP Conf. Ser.: Mater. Sci. Eng.* **95** 012111.
[19] Liu S B, Wang Q and Liu G 2000 *Wear* **243** 101
[20] Polonsky I A and Keer L M 1999 *Wear* **231** 206